Supporting Information

Target-induced nanocatalyst deactivation facilitated by core@shell nanostructures for signal-amplified headspace-colorimetric assay of dissolved hydrogen sulfide

Zhuangqiang Gao,[†] Dianyong Tang,[‡] Dianping Tang,*[,†] Reinhard Niessner,[§] and Dietmar Knopp[§]

[†]Institute of Nanomedicine and Nanobiosensing, Key Laboratory of Analysis and Detection for Food Safety (Fujian Province & Ministry of Education), Department of Chemistry, Fuzhou University, Fuzhou 350108, China

[‡]Chongqing Key Laboratory of Environmental Materials & Remediation Technologies, College of Materials and Chemical Engineering, Chongqing University of Arts and Sciences, Chongqing 402160, China

[§]Chair for Analytical Chemistry, Institute of Hydrochemistry, Technische Universität München, Marchioninistrasse 17, D-81377 München, Germany

E-mail: dianping.tang@fzu.edu.cn (D. Tang)

Fax: +86 591 2286 6135; Tel.: +86 591 2286 6125.

Table of Contents

A. Experimental Section

A1. Materials and reagents.

3,3',5,5'-Tetramethylbenzidine (TMB), chloroauric acid tetrahydrate ($HAuCl_4 \cdot 4H_2O$, 99.9 %) and hexachloroplatinic acid hexahydrate ($H_2PtCl_6 \cdot 6H_2O$, 99.9 %) were purchased from Sinopharm Chem. Re. Co., Ltd. (Shanghai, China). Sodium citrate tribasic dihydrate was acquired from Sigma-Aldrich (St. Louis, MO). L-Ascorbic acid (AA) was obtained from Fluka (USA). Sodium sulfide ($Na_2S \cdot 9H_2O$, 98%) and hydrogen peroxide (H_2O_2, 30%) were purchased from Aladdin (Shanghai, China). All other reagents and chemicals were of analytical grade at least. Ultrapure water (18.2 MΩ cm^{-2}) obtained from Milli-Q water purification system (Millipore) was used throughout the experiments. A 0.1 M phosphate-buffered saline (PBS, pH 6.0) was prepared by adding 0.44 g $Na_2HPO_4 \cdot 12H_2O$ and 1.37 g $NaH_2PO_4 \cdot 2H_2O$ in 100-mL ultrapure water, and the substrate solution for Pt nanostructures was prepared by adding 0.921 mM TMB and 7.5 M H_2O_2 in citrate acid-phosphate buffer (pH 4.0).

A2. Preparation of (gold core)@(platinum shell) nanoparticles (Au@PtNPs) with various Pt shell thicknesses.

The Au@PtNPs with 2 monolayer-equivalents of Pt (θ_{Pt} = 2, Au@TPt-NCs) were prepared following the reported seed-mediated protocol with slight modification [*Note*: Because the growth of Pt on Au surface follows Volmer–Weber growth mode, Pt grows as a set of clusters, and not as a set of continuous monolayers on Au surface, but we will utilize monolayer-equivalents (denoted as θ_{Pt}) to approximately describe the Pt amount on each nanoparticle].[S1,S2] In brief, gold nanoparticles (AuNPs, ~16 nm) were first synthesized *via* reduction of $HAuCl_4$ by sodium citrate using the classical Frens' method and employed as the cores. Then, 15 mL of the as-prepared AuNPs solution, 0.112 mL of 10 mM H_2PtCl_6 solution and 9.328 mL H_2O were mixed together, and the obtained solution was heated to 80 °C under stirring. Following that, 0.560 mL of 10 mM AA

solution was added drop-wise slowly into the above solution by a step-motor driven syringe, along with continuous stirring. The mixture was then reacted for another 30 min, and its color turned from red to orange-red, indicating the formation of Au@PtNPs (θ_{Pt} = 2). For the preparation of Au@PtNPs with other Pt shell thicknesses (θ_{Pt} = 1, 3, 4, 5, 6, 8, 10, 15), the volumes of the used H_2PtCl_6 solution and AA solution were changed while the volume of AuNPs solution was constant based on the following relation:

$$D = D_{core} (1 + (V_{m,Pt} N_{Pt}) / (V_{m,Au} N_{Au}))^{1/3}$$

where D and D_{core} are the diameters of the AuNPs and Au@PtNPs, $V_{m,Au}$ and $V_{m,Pt}$ are the molar volumes of the Au and Pt, and N_{Au} and N_{Pt} are the number of moles of the used Au and Pt, respectively (see the detailed dosages of H_2PtCl_6 solution and AA solution in the following Table S1). During this process, these as-prepared nanoparticles were characterized by transmission electron microscopy (TEM; TECNAI G2F20, FEI; Figure 1A,B and Figure 3A-H). Moreover, the particle concentrations of the as-prepared AuNPs and Au@PtNPs solutions were calculated to be 2.32 and 1.39 nM, respectively (see the detailed calculation process in Part C1 in Supporting Information).

Table S1. The dosages of materials for the preparation of Au@PtNPs with different Pt shell thicknesses.

Pt shell thickness (θ_{Pt})	Volume of AuNP colloid / mL	Volume of H_2O / mL	Volume of 10mM H_2PtCl_6 solution / mL	Volume of 10 mM AA solution / mL
1	15	9.676	0.054	0.270
2	15	9.328	0.112	0.560
3	15	8.962	0.173	0.865
4	15	8.566	0.239	1.195
5	15	8.152	0.308	1.540
6	15	7.708	0.382	1.910
8	15	6.742	0.543	2.715
10	15	5.662	0.723	3.615
15	15	2.434	1.261	6.305

A3. Preparation of platinum nanoparticles (PtNPs).

The PtNPs used in this study were prepared according to the previous reports.[S3,S4] Briefly, 100 mL of 0.01% (w/v) $H_2PtCl_6 \cdot 6H_2O$ aqueous solution was heated to boil under vigorous stirring, followed by the addition of 1 mL of 3% sodium citrate solution. After half a minute, 1mL of a freshly prepared solution containing 0.08% $NaBH_4$ and 1% sodium citrate was quickly added into the mixture. The obtained mixture was kept boiling and stirring for 30 min, and then turned champagne. The average diameter of the prepared PtNPs was 3.5 nm based on the TEM characterization (Figure S3). And the particle concentration of the PtNPs solution was calculated to be 130 nM (see the detailed calculation process in Part C2 in Supporting Information).

A4. The Au@TPt-HCA method for detecting dissolved H_2S.

The operational flowchart of the Au@TPt-HCA method was displayed in Figure S1 (Part B1 in Supporting Information). Before measurement, H_2S standards with various concentrations were initially prepared by using Na_2S as the source and 0.1 M phosphate-buffered saline (PBS, pH 6.0) as the sample matrix based on the reported literature.[S5] Afterward, 300 μL of H_2S standards or samples was added into the bottom of a 0.5-mL Eppendorf tube, and 3 μL of 69.5 pM Au@TPt-NCs solution was pipetted onto the internal side of the cap of the tube. Then the above tube was sealed immediately by closing the Au@TPt-NCs-coated cap, and incubated for 30 min at room temperature (RT, 25±1 °C). Subsequently, the Au@TPt-NCs-coated cap was opened, and 100 μL of the substrate solution was added to the cap and incubated for 10 min at RT. Finally, the absorbance of the resulting solution (90 μL) was measured at 650 nm by a microplate reader (Tecan Infinite 200 PRO, TECAN, Switzerland).

A5. Feasibility of the Au@TPt-HCA method for detecting dissolved H_2S.

(1). The feasible study of H_2S-induced deactivation of Au@TPt-NCs: (i) 3 μL of 69.5 pM Au@TPt-NCs solution was mixed with 10μL of H_2S aqueous solution with different concentrations (0, 100, 500, and 1000 nM) in a 0.5-mL Eppendorf tube, and the obtained mixture was incubated for 30 min at RT; (ii) 100 μL of the substrate solution was added to the mixture and incubated for 10 min at RT; and (iii) the absorbance of the final solution (100 μL) was measured at 650 nm by a microplate reader (Tecan Infinite 200 PRO, TECAN, Switzerland).

(2). The feasible study of the integration of H_2S-induced deactivation of Au@TPt-NCs with static headspace strategy: (i) 300 μL of H_2S aqueous solution with different concentrations (0, 100, 200, and 500 nM) was added into the bottom of a 0.5-mL Eppendorf tube, and 3 μL of 69.5 pM Au@TPt-NCs solution was pipetted onto the underside of the cap of the tube; (ii) the above tube was sealed immediately by closing the cap, and incubated for 30 min at RT; (iii) the cap was opened, and 100 μL of the substrate solution was added to the cap and incubated for 10 min at RT; and (iv) the absorbance of the resulting solution (90 μL) was measured at 650 nm by a microplate reader (Tecan Infinite 200 PRO, TECAN, Switzerland).

A6. Advantages of the static headspace strategy for the Au@TPt-HCA method

(1). the Au@TPt-HCA method with static headspace strategy: (i) 300 μL of H_2S aqueous solution (0 and 100 nM) in different complex aqueous mediums (10% (w/w) NaCl, 1% (w/w) bovine serum albumin (BSA), 1 mM cetyltrimethylammonium bromide (CTAB), and 1 mM cysteine (Cys)) was added into the bottom of a 0.5-mL Eppendorf tube, and 3 μL of 69.5 pM Au@TPt-NCs solution was pipetted onto the underside of the cap of the tube; (ii) the above tube was sealed immediately by closing the cap, and incubated for 30 min at RT; (iii) the cap was opened, and 100 μL of the substrate solution was added to the cap and incubated for 10 min at RT; and (iv) the absorbance of the resulting solution (90 μL) was measured at 650 nm by a microplate reader (Tecan Infinite 200 PRO, TECAN, Switzerland).

(2) the Au@TPt-HCA method without static headspace strategy: (i) 3 μL of 69.5 pM Au@TPt-NCs solution was mixed with 10μL of H_2S aqueous solution (0 and 100 nM) in different complex aqueous mediums (10% (w/w) NaCl, 1% (w/w) bovine serum albumin (BSA), 1 mM cetyltrimethylammonium bromide (CTAB), and 1 mM cysteine (Cys)), and the obtained mixture was incubated for 30 min at RT; (ii) 100 μL of the substrate solution was added to the mixture and incubated for 10 min at RT; and (iii) the absorbance of the final solution (100 μL) was measured at 650 nm by a microplate reader (Tecan Infinite 200 PRO, TECAN, Switzerland).

A7. Advantages of Au@TPt-NCs for H_2S-induced nanocatalyst deactivation.

Initially, 300 μL of H_2S standards (0 and 50 nM in PBS (pH 6.0)) was added into the bottom of a 0.5-mL Eppendorf tube, and 3 μL of Pt/Au nanoparticles solution with the same total surface area

was pipetted onto the underside of the cap of the tube (see the following Table S2 for the detailed dosages of the used Pt/Au nanoparticles). Then the above tube was sealed immediately by closing the cap, and incubated for 30 min at RT. Subsequently, the cap was opened, and 100 μL of the substrate solution was added to the cap and incubated for 10 min at RT. Finally, the absorbance of the resulting solution (90 μL) was measured at 650 nm by a microplate reader (Tecan Infinite 200 PRO, TECAN, Switzerland).

Table S2. The dosages of used Pt/Au nanoparticles with the same surface area.

Pt/Au nanoparticles	Mean size of nanoparticles / nM	Suface area of a nanoparticle / nM^2	The used particle concentration / pM	The used volume of nanoparticles / μL
AuNPs	15.8	784.3	81.4	3
PtNPs	3.5	38.5	1658.9	3
Au@PtNPs (θ_{Pt} = 1)	16.5	855.3	74.6	3
Au@PtNPs (θ_{Pt} = 2, *i.e.*, Au@TPt-NCs)	17.1	918.6	69.5	3
Au@PtNPs (θ_{Pt} = 3)	17.8	995.4	64.1	3
Au@PtNPs (θ_{Pt} = 4)	18.6	1086.9	58.7	3
Au@PtNPs (θ_{Pt} = 5)	19.7	1219.2	52.4	3
Au@PtNPs (θ_{Pt} = 6)	20.9	1372.3	46.5	3
Au@PtNPs (θ_{Pt} = 8)	24.7	1916.7	33.3	3
Au@PtNPs (θ_{Pt} = 10)	29.9	2808.6	22.7	3
Au@PtNPs (θ_{Pt} = 15)	35.0	3848.5	16.6	3

Note: The used particle concentration is dependent on the corresponding surface area of a nanoparticle to ensure the comparison study under the same total surface area.

A8. Computational details.

All of the DFT calculations were carried out using the Cambridge Serial Total Energy Package (CASTEP) codes.[S6] An ultrasoft pseudopotential was chosen to deal with the interaction between ion cores and valence electrons. The exchange-correlation effects between valence electrons were described by the Perdew−Burke−Ernzerhof (PBE) functional using the generalized gradient approximation (GGA).[S7] The Kohn−Sham wave functions for the valence electrons were expanded using a plane-wave basis set within an energy cutoff of 320 eV. The energy cutoff was increased to 400 eV to test for convergence, and the d-band centers were found to vary by less than 0.01 eV. The

Monkhorst−Pack scheme K-points grid sampling was set as 4 × 4 × 1 for the irreducible Brillouin zone. The Broyden−Fletcher−Goldfarb−Shanno (BFGS) scheme was chosen as the minimization algorithm.[S8] Its iterative process was considered to be converged when the force on the atoms was less than 0.03 eV/Å, the stress on the atoms was less than 0.05 GPa, the atomic displacement was less than 1×10^{-3} Å, and the energy change per atom was less than 1×10^{-5} eV.

We first calculated the bulk crystal structure of Au and Pt, which gave the following lattice parameters: a = b = c = 4.1931 (Au)/3.9988 (Pt) Å. This is in good agreement with the experimental parameters: a = b = c = 4.0783 (Au) / 3.9239 (Pt) Å. The Au(111) and Pt(111) were simulated by the periodic (2 × 2) slab models. These models have six atomic layers. The slabs were separated by a 20 Å thick vacuum, which is sufficient to screen the self-interaction effects of the periodic boundary conditions. Au@TPt-NCs were modeled with different Pt monolayers (1, 2, 3, 4, 5, 6, 7, 11) on the p (2 × 2) Au(111) slabs with the six atomic layers. The p (2 × 2) Pt(111) monolayers were constrained in the p (2 × 2) Au(111) surface. The atomic positions of the bottom four atomic layers were fixed to simulate the bulk effects.

B. Additional Results and Disscussion

B1. Additional Figures.

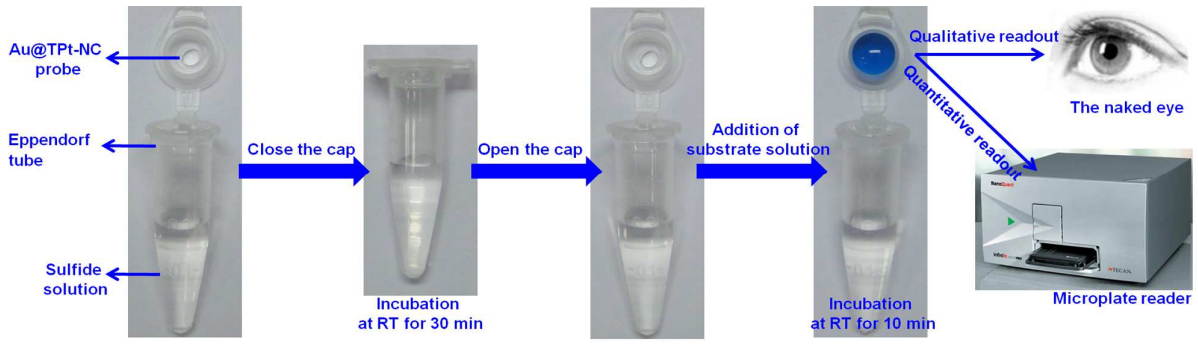

Figure S1. Operational flowchart of the developed Au@TPt-HCA method for the detection of dissolved H_2S.

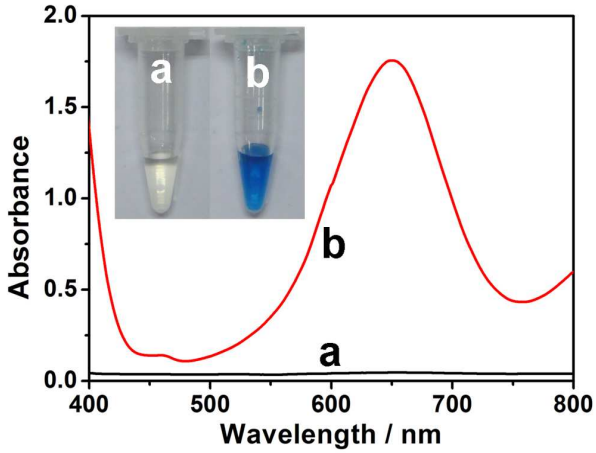

Figure S2. UV-vis absorption spectra of (a) H_2O_2-TMB and (b) Au@TPt-NCs + (H_2O_2-TMB) (*Insets*: the corresponding photographs). The experiments were carried out using 10 μL of Au@TPt-NCs (60-times dilution from stock solutions) in 100-μL substrate solution (0.921 mM TMB and 7.5 M H_2O_2 in citrate acid-phosphate buffer (pH 4.0)) at RT for 10 min, and the UV-vis absorption spectra were measured by a microplate reader (Tecan Infinite 200 PRO, TECAN, Switzerland).

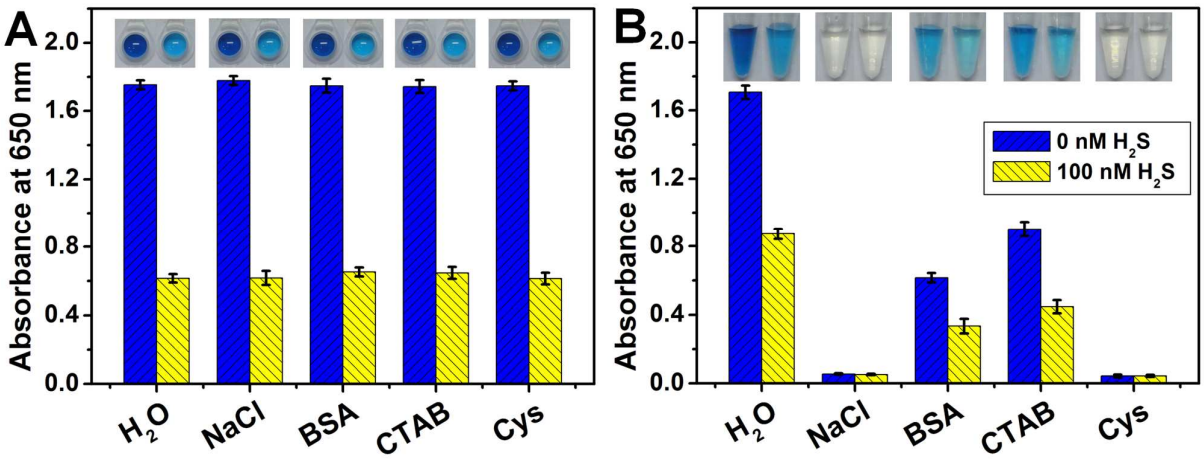

Figure S3. Comparison study of the Au@TPt-HCA method in the (A) presence and (B) absence of the static headspace strategy for the detection of 0 nM (blue column) and 100 nM (yellow column) H_2S in water and some complex aqueous mediums (10% NaCl, 1%BSA, 1 mM CTAB, and 1 mM Cys), respectively (*Inserts*: the corresponding photographs). Error bar represents the standard deviation (n = 3).

Advantages of the static headspace strategy for the Au@TPt-HCA method.

In the practical applications, some detection mediums for dissolved H_2S are very complex, *e.g.*, high-salinity (~3.5%) in sea water, present of proteins and other biological thiols in blood/serum,

and uncertain interferents (*e.g.*, surfactants) in wastewater. To demonstrate the advantages of the static headspace strategy, the Au@TPt-HCA method was used to detect dissolved H_2S (100 nM as an example) with and without the static headspace strategy in some complex aqueous mediums (*e.g.*, 10% (w/v) NaCl solution, 1% (w/v) bovine serum albumin (BSA) solution, 1 mM cetyltrimethylammonium bromide (CTAB) solution, and 1 mM cysteine (Cys) solution), and the results were compared with those in pure water condition. As shown in Figure S3A, in the presence of the static headspace strategy, the assay results in the complex aqueous mediums were almost the same as those in pure water, indicating that these complex aqueous mediums had no obvious influence for H_2S sensing by using the static headspace strategy. In contrast, in the absence of the static headspace strategy, the assay results in the complex aqueous mediums were much worse than those in pure water, showing the disadvantages of the analytical system without the static headspace strategy (Figure S3B). These results demonstrated that the use of the static headspace strategy could greatly improve the selectivity and anti-jamming capability of the assay system, thereby enhancing the accuracy and precision of the analytical results.

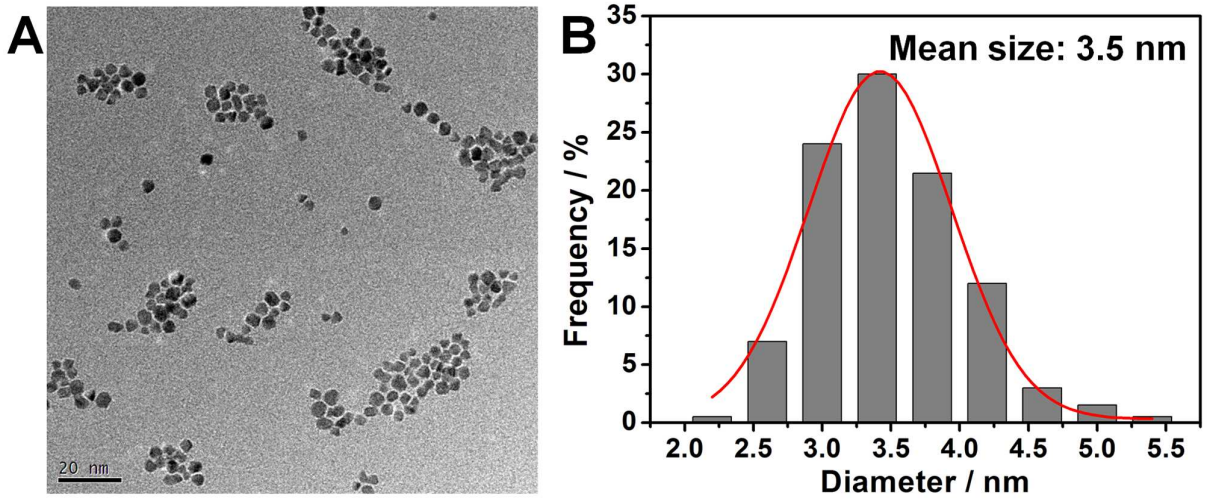

Figure S4. (A) TEM image and (B) size distribution of the as-prepared PtNPs used in this study.

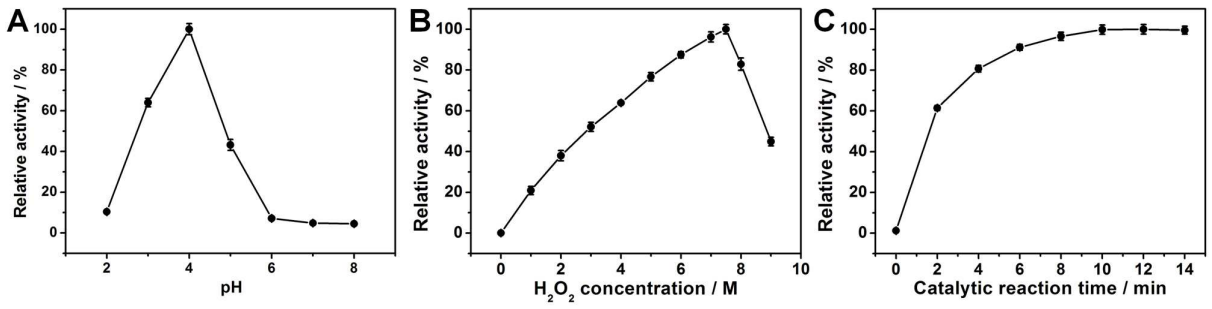

Figure S5. Effects of (A) pH of citrate acid-phosphate buffer, (B) H_2O_2 concentration and (C) incubation time on the peroxidase-like catalytic activity of Au@TPt-NCs. Error bars indicate standard deviations (n = 3). Experiments were carried out by using 3-μL Au@TPt-NCs (69.5 pM) in 100-μL substrate solution (0.921 mM TMB and 7.5 M H_2O_2 in citrate acid-phosphate buffer (pH 4.0)) at RT for 10 min under different pH values, H_2O_2 concentrations and incubation times, respectively. The absorbance was read at 650 nm with a microplate reader (Tecan Infinite 200 PRO, TECAN, Switzerland). The detail conditions were as follows: (A) pH value: from 2 to 8, H_2O_2 concentration: 1.0 M, Temperature: 25°C; (B) H_2O_2 concentration: from 0 to 9 M, pH = 4.0, Temperature: 25°C; (C) Incubation time: from 0 to 14 min, pH = 4.0, H_2O_2 concentration: 7.5 M, Temperature: 25°C. The maximum point in each curve was set as 100%.

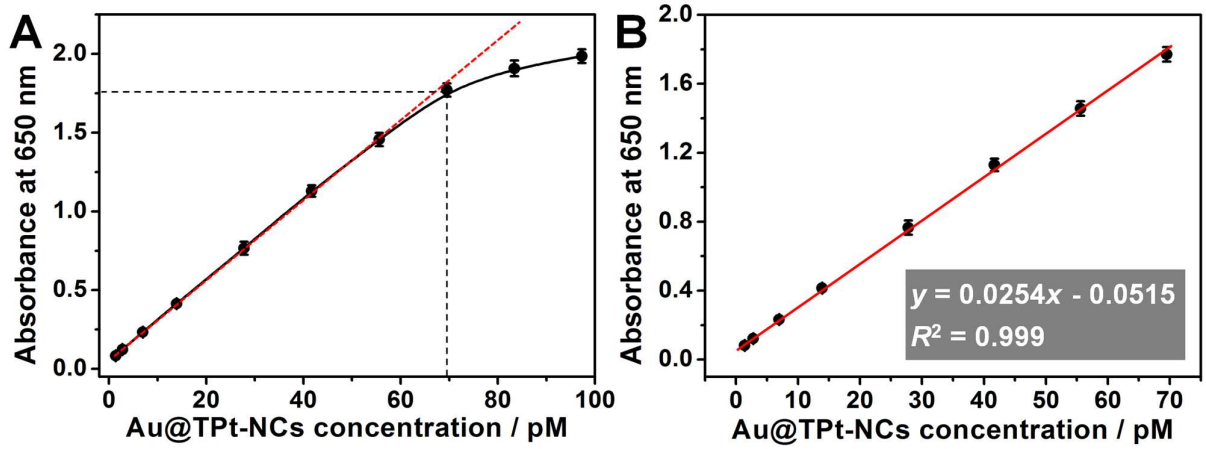

Figure S6. (A) Au@TPt-NCs concentration-dependent absorbance response of Au@TPt-NCs+(H_2O_2-TMB) catalytic system, and (B) the corresponding linear curve. Error bars indicate standard deviations (n = 3). Experiments were carried out by using 3-μL Au@TPt-NCs with different concentrations in 100-μL substrate solution (0.921 mM TMB and 7.5 M H_2O_2 in citrate acid-phosphate buffer (pH 4.0)). The absorbance was read at 650 nm with a microplate reader (Tecan Infinite 200 PRO, TECAN, Switzerland).

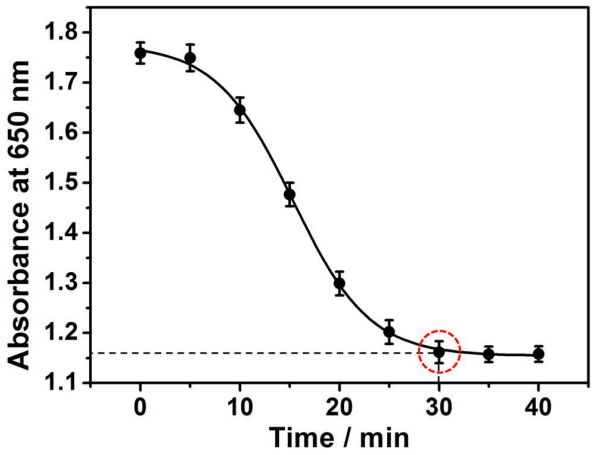

Figure S7. Time-dependent absorbance response of Au@TPt-NCs+(H_2O_2-TMB) catalytic system toward 50 nM H_2S. Error bars indicate standard deviations (n = 3). Experiments were carried out as followings: 300 μL of 50 nM H_2S was added into the bottom of a 0.5-mL Eppendorf tube, and 3 μL of 69.5 pM Au@TPt-NCs solution was pipetted onto the underside of the cap of the tube, then the above tube was sealed immediately by closing the cap, and incubated for different time (0, 5, 10, 15, 20, 25, 30, 35, and 40 min) at RT, subsequently, the cap was opened, and 100 μL of substrate solution (0.921 mM TMB and 7.5 M H_2O_2 in citrate acid-phosphate buffer (pH 4.0)) was added to the cap and incubated for 10 min at RT. Meanwhile, the absorbance was measured at 650 nm by a microplate reader (Tecan Infinite 200 PRO, TECAN, Switzerland).

Optimization of experimental conditions.

To achieve an optimal colorimetric signal for detecting H_2S, some experimental parameters including operational temperature, catalytic conditions of Au@TPt-NCs for H_2O_2-TMB system, and Au@TPt-NCs concentration and incubation time for H_2S+Au@TPt-NCs reaction, which greatly influenced the analytical performance of the developed method, should be optimized. In order to facilitate the convenient application of the developed method for future detection, room temperature (RT, 25±1 °C) was selected as the operational temperature for all measurements and incubations throughout the experiment. In this work, the colorimetric signal originated from the peroxidase-like catalytic activity of Au@TPt-NCs, so their catalytic conditions for H_2O_2-TMB system were very important for obtaining the best colorimetric signal. As seen from Figure S5, the catalysis of Au@TPt-NCs toward H_2O_2-TMB system could be better carried out as follows: effective working pH of 4.0, effective H_2O_2 concentration of 7.5 M, and effective incubation time of 10 min, which was similar with the platinum nanostructures studied in our previous reports.[S9,S10]

Clearly, the concentration of Au@TPt-NCs solution used in this experiment was a key factor for this colorimetric assay. To choose a suitable concentration of Au@TPt-NCs, the relationship between absorbance (at 650 nm) of Au@TPt-NCs+(H_2O_2-TMB) catalytic system and Au@TPt-NCs concentration was studied (Figure S6). Typically, the absorbance increased proportionally with the increase of Au@TPt-NCs concentration in the range from 1.39 to 69.5 pM, and then the increasing tendency slowed down when the Au@TPt-NCs concentration was higher than 69.5 pM. That is to say, the absorbance of Au@TPt-NCs+(H_2O_2-TMB) catalytic system was sensitive to the change of Au@TPt-NCs concentration from 1.39 to 69.5 pM, but relatively insensitive to the change of Au@TPt-NCs concentration higher than 69.5 pM. As mentioned in H_2S-induced deactivation of Au@TPt-NCs, H_2S could cause the deactivation of Au@TPt-NCs, leading to the decrease of the activated Au@TPt-NCs concentration, which pave a way for indicating the corresponding H_2S concentration. Thus, when the Au@TPt-NCs concentration was higher than 69.5 pM, the absorbance of Au@TPt-NCs+(H_2O_2-TMB) system would be insensitive to the addition of H_2S (which equalled to the decrease of the Au@TPt-NCs concentration). Therefore, 69.5 pM was used as the concentration of Au@TPt-NCs for H_2S+Au@TPt-NCs reaction in this work.

In addition, the incubation time for H_2S+Au@TPt-NCs reaction directly affects the deactivation degree of Au@TPt-NCs. As indicated from Figure S7, the colorimetric signal decreased with the increment of reaction time and reached to the steady-state signal after 30 min (50 nM H_2S as an example). Longer reaction time did not cause obvious decrease in the colorimetric signal. Hence, a reaction time of 30 min was selected for the H_2S+Au@TPt-NCs reaction in this study.

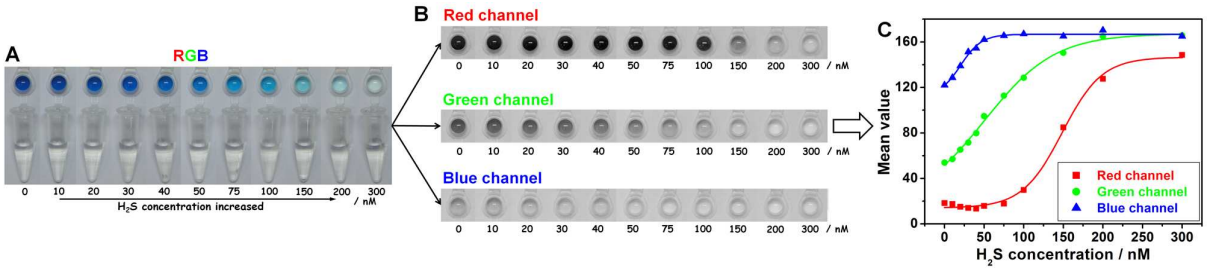

Figure S8. Schematic illustration of the RGB values to analyze the color change by using digital camera images. (A) Image of colorimetric response of the Au@TPt-HCA method toward H_2S standards with different concentrations, (B) red, green and blue channels from original image (A) to different concentration of H_2S

processed using Adobe Photoshop CS5 software, and (C) Mean values of red, green and blue channels obtained from original image (A) to different concentration of H_2S.

B2. Additional Tables.

Table S3. Comparison of the LOD of various established methods for the detection of dissolved H_2S

Method	Probe	LOD / nM	references
Colorimetric method	Methylene blue	2000	S11
	Ag^+ ion	8700	S12
	Glutathione-modified gold nanoparticle	3000	S13
	Au/Ag core/shell nanorods	500	S14
	Cu@Au nanoparticles	300	S15
	Nitrobenzofurazan (7-nitro-1,2,3-benzoxadiazole) thioethers	190	S16
	Bare gold nanoparticles	80	S17
	Au−Ag core−shell nanoparticles	50	S18
Fluorescence	SulpHensor	500	S19
	Responsive lanthanide coordination polymer	300	S20
	TFCA	86	S21
	Thiolysis of dinitrophenyl ether	50	S22
	Intermolecular thiolysis of dinitrophenyl ether	48	S23
	6-(benzo[d]thiazol-2'-yl)-2-azidonaphthalene	20	S24
	HS–Cy	5-10	S25
	Gold/silver nanoclusters	0.830	S26
Luminescence	Cy2-MSNs/Ir1	2700	S27
	UCNPs@mSiO2-MC	580	S28
	A Eu(III) complex	80	S29
	$[Ru(bpy)_2(phen\text{-}cyc)Cu](PF_6)_4$	21.6	S30
	MPA-CdTe QDs-Cy-N_3	7	S31
	[4'-(2,4-dinitrophenyloxy)-2,2':6',2''-terpyridine-6,6''-diyl]bis(methylenenitrilo) tetrakis(acetate)-Eu^{3+}/Tb^{3+}	3.5	S32
Electrochemical method	Dimethyl-*p*-phenylenediamine	7500	S33

	Diethyl-*p*-phenylenediamine	4000	S34
	A thin silicone membrane + ferricyanide	2000	S35
	Boron doped diamond flow electrodes	370	S36
	Carbon nanotube modified glassy carbon electrodes	300	S37
	H_2S permeable membrane + ferricyanide	10	S38
	DNA-based polyion complex membrane + Hg^{2+}	0.35	S5
Colorimetric method	Au@TPt-NCs	7.5	This work

Table S4. The water quality standards for sulfide level in various waters according to the State Standard of the People's Republic of China.

Waters	Sulfide concentration / mg L^{-1}	Sulfide concentration / μM	Water quality standards
Wastewater	≤ 1	≤ 31	Integrated Wastewater Discharge Standard (GB 8978-1996)
Drinking water	≤ 0.02	≤ 0.63	Standards for drinking water quality (GB 5749-2006)
Aquaculture water	≤ 0.2	≤ 6.3	Water quality standards for fisheries (GB 11607-89)
Irrigation water	≤ 1.0	≤ 31	Standards for irrigation water quality (GB 5084-92)
Sea water (class-I criteria)	≤ 0.02	≤ 0.63	Sea water quality standard (GB 3097-1997)
Sea water (class-II criteria)	≤ 0.05	≤ 1.56	Sea water quality standard (GB 3097-1997)
Sea water (class-III criteria)	≤ 0.10	≤ 3.1	Sea water quality standard (GB 3097-1997)
Sea water (class-IV criteria)	≤ 0.25	≤ 7.8	Sea water quality standard (GB 3097-1997)
Surface water (class-I criteria)	≤ 0.05	≤ 1.56	Environmental quality standards for surface water (GB 3838-2002)
Surface water (class-II criteria)	≤ 0.10	≤ 3.1	Environmental quality standards for surface water (GB 3838-2002)

Surface water (class-III criteria)	≤ 0.20	≤ 6.3	Environmental quality standards for surface water (GB 3838-2002)
Surface water (class-IV criteria)	≤ 0.50	≤ 15.6	Environmental quality standards for surface water (GB 3838-2002)
Surface water (class-V criteria)	≤ 1.0	≤ 31	Environmental quality standards for surface water (GB 3838-2002)

Table S5. Assessment of the material expense for a typical preparation of Au@TPt-NCs.

Chemical	Molecular weight / g mol^{-1}	Concentration / mol L^{-1}	Volume / L	Price / US$ g^{-1}	Expense / US$
$HAuCl_4$ $4H_2O$	411.85	2.94×10^{-4}	1.50×10^{-2}	61.130	0.111
$C_6H_5Na_3O_7$ $2H_2O$	294.10	3.88×10^{-2}	3.00×10^{-4}	0.068	2.328×10^{-4}
H_2PtCl_6 $6H_2O$	517.90	0.01	1.12×10^{-4}	54.572	0.032
AA	176.12	0.01	5.60×10^{-4}	0.379	3.738×10^{-4}
Total					0.143

Note: The prices are found from the corresponding reagent companies, and calculated according to the price of the bulkiest package of each chemical.

Table S6. Assessment of material expense for a typical process of the Au@TPt-HCA method

Chemical	Molecular weight / g mol^{-1}	Concentration / mol L^{-1}	Volume / L	Price / US$ g^{-1}	Expense / US$
H_2O_2	34.01	7.50	1.00×10^{-4}	0.047	1.208×10^{-3}
TMB	240.35	9.21×10^{-4}	1.00×10^{-4}	16.034	3.549×10^{-4}
Buffer solution					1.066×10^{-5}
Au@TPt-NCs					8.580×10^{-7}
Total					1.574×10^{-3} ≈ 0.002

Note: The prices are found from the corresponding reagent companies, and calculated according to the price of the bulkiest package of each chemical.

Cost evaluation for a single test with the Au@TPt-HCA method.

Here we only evaluated the reagents' cost involved in the work for a single test of one sample, and the consumption for power, labor, and depreciation of instruments were not taken into account. During the preparation of Au@TPt-NCs, the expense of the used chemicals for a typical preparation of Au@TPt-NCs was estimated in Table S5. According to this recipe (Table S5), 25 mL of Au@TPt-NCs colloids with a particle concentration of 1.39 nM could be obtained. Thus, the expense of 3-μL Au@TPt-NCs colloids with a particle concentration of 69.5 pM was US$8.58 × 10^{-7}, which was negligible. Then the expense of the materials for a single test was estimated in Table S6. As seen from Table S6, the whole expense for one sample test was roughly US$0.002.

Table S7. Reproducibility and precision of the Au@TPt-HCA method.

Item	*c* [H_2S] / nM	Absorbance at 650 nm						Mean±SD, *n* = 6	CV / %, *n* = 6
		1	2	3	4	5	6		
Intra-assay	20	1.6024	1.6540	1.6472	1.5528	1.5684	1.6196	1.6074±0.0411	2.6
	50	1.1694	1.1105	1.0946	1.1108	1.1984	1.2148	1.1498±0.0512	4.4
	100	0.5475	0.6091	0.6125	0.5210	0.5526	0.5126	0.5592±0.0427	7.6
Inter-assay	20	1.4989	1.6277	1.6511	1.5059	1.6054	1.6324	1.5869±0.0671	4.2
	50	1.0805	1.1494	1.2088	1.1086	1.0997	1.1767	1.1373±0.0495	4.3
	100	0.5186	0.5412	0.6918	0.5475	0.5841	0.6728	0.5927±0.0728	12.3

Reproducibility and precision of the Au@TPt-HCA method.

The reproducibility and precision of the Au@TPt-HCA method were investigated by using different batches of Au@TPt-NCs for the detection of three H_2S standards with different concentrations (20, 50 and 100 nM H_2S). Experimental results indicated that the coefficients of variation (CVs) of the intra-assay using the same-batch Au@TPt-NCs were 2.6~7.6% (n = 6), whereas the CVs of the inter-assay with different batches were 4.2~12.3% (n = 6), respectively (Table S7). These results revealed that the reproducibility and precision of the developed Au@TPt-HCA method were acceptable.

Table S8. Recovery evaluation by using Na_2S as the donor to spike 4 blank sample matrices containing local top water, Minjiang river water, local sea water and newborn cattle serum by using the developed Au@TPt-HCA method.

Substrate	Sample no. [a]	Spiked / nM	Found (mean ± SD) / nM	Recovery / %
Top water	1	20	18.6 ± 1.4	93.0
	2	40	41.0 ± 1.7	102.5
	3	60	62.7 ± 3.0	104.4
	4	80	77.1 ± 2.5	96.4
Minjiang river water	5	20	21.3 ± 1.2	106.7
	6	40	37.7 ± 2.2	94.3
	7	60	61.5 ± 1.9	102.5
	8	80	76.2 ± 3.1	95.3
Sea water	9	20	21.1 ± 2.7	105.3
	10	40	41.5 ± 2.2	103.8
	11	60	58.4 ± 2.5	97.3
	12	80	74.5 ± 3.2	93.1
Newborn cattle serum	13	20	18.3 ± 2.5	91.6
	14	40	38.2 ± 2.2	95.5
	15	60	56.2 ± 4.0	93.6
	16	80	77.7 ± 3.3	97.1

[a] Each sample was assayed in triplicate.

C. Calculation Processes

C1. Calculation process of the concentrations of the as-prepared AuNPs solution and Au@PtNPs solution.

Known conditions:

1) the diameter of AuNPs used in this study: d_{AuNP} = 16 nm,

2) the density of gold: ρ_{Au} = 19.32 g cm^{-3},

3) the concentration of $HAuCl_4$ solution used for preparing AuNPs: $c_{HAuCl4} = 2.94 \times 10^{-4}$ mol L^{-1},

4) the volume of $HAuCl_4$ solution used for preparing AuNPs: V_{HAuCl4} = 100 mL,

6) the molar mass of gold: M_{Au} = 197 g mol^{-1},

7) the Avogadro constant: $N_A = 6.02 \times 10^{23}$.

Then, the volume of an AuNP with a diameter of 16 nm is

$V_{an\ AuNP} = 4/3\ \pi\ (d_{AuNP} / 2)^3 = 4 / 3 \times 3.14 \times (16\ nm / 2)^3 = 2.144 \times 10^3\ nm^3 = 2.144 \times 10^{-18}\ cm^3$

The mass of an AuNP with a diameter of 16 nm is

$m_{an\ AuNP} = \rho_{Au}\ V_{an\ AuNP} = 19.32\ g\ cm^{-3} \times 2.144 \times 10^{-18}\ cm^3 = 4.142 \times 10^{-17}\ g$

The total mass of gold in 100 mL $HAuCl_4$ solution used for preparing AuNPs is

$m_{total\ Au} = n_{Au}\ M_{Au} = c_{HAuCl4}\ V_{HAuCl4}\ M_{Au} = 2.94 \times 10^{-4}\ mol\ L^{-1} \times 100\ mL \times 197\ g\ mol^{-1} = 5.792 \times 10^{-3}\ g$

The number of 16 nm AuNPs prepared from 100 mL $HAuCl_4$ solution based on the complete transformation of $HAuCl_4$ to AuNPs is

$N_{AuNPs} = m_{total\ Au} / m_{an\ AuNP} = 5.792 \times 10^{-3}\ g / 4.142 \times 10^{-17}\ g = 1.398 \times 10^{14}$

The amount of 16 nm AuNPs prepared from 100 mL $HAuCl_4$ solution is

$n_{AuNPs} = N_{AuNPs} / N_A = 1.398 \times 10^{14} / 6.02 \times 10^{23} = 2.32 \times 10^{-10}\ mol$

The particle concentration of 16 nm AuNPs prepared from 100 mL $HAuCl_4$ solution is

$c_{AuNPs} = n_{AuNPs} / V_{HAuCl4} = 2.32 \times 10^{-10}\ mol / 100\ mL = 2.32 \times 10^{-9}\ mol\ L^{-1} = 2.32\ nmol\ L^{-1} = 2.32\ nM$

Since the Au@PtNPs with different Pt shell thicknesses (25 mL) were all prepared by using 16 nm AuNPs (15 mL) as cores, thus the concentrations of these prepared Au@PtNPs are the same:

$c_{Au@PtNPs} = 15 / 25\ c_{AuNPs} = 15 / 25 \times 2.32\ nM = 1.39\ nM$

So, the particle concentrations of the synthesized AuNPs solution and Au@PtNPs solution were 2.32 and 1.39 nM, respectively.

C2. Calculation process of the concentration of the as-prepared PtNPs solution.

Known conditions:

1) the diameter of PtNPs used in this study: d_{PtNP} = 3.5 nm,

2) the density of platinum: ρ_{Pt} = 21.45 g cm^{-3},

3) the concentration of $H_2PtCl_6 \cdot 6H_2O$ solution used for preparing PtNPs: $c_{H2PtCl6 \cdot 6H2O}$ = 0.0001 g mL^{-1} (w/v),

4) the volume of $H_2PtCl_6 \cdot 6H_2O$ solution used for preparing PtNPs: $V_{H2PtCl6 \cdot 6H2O}$ = 100 mL,

6) the molar mass of platinum: M_{Pt} = 195.05 g mol^{-1},

7) the molar mass of $H_2PtCl_6 \cdot 6H_2O$: $M_{H2PtCl6 \cdot 6H2O}$ = 517.92 g mol^{-1},

8) the Avogadro constant: $N_A = 6.02 \times 10^{23}$.

Then, the volume of an PtNP with a diameter of 3.5 nm is

$V_{\text{an PtNP}} = 4/3\ \pi\ (d_{\text{PtNP}} / 2)^3 = 4 / 3 \times 3.14 \times (3.5\ \text{nm} / 2)^3 = 22.45\ \text{nm}^3 = 2.245 \times 10^{-20}\ \text{cm}^3$

The mass of an PtNP with a diameter of 3.5 nm is

$m_{\text{an PtNP}} = \rho_{\text{Pt}}\ V_{\text{an PtNP}} = 21.45\ \text{g cm}^{-3} \times 2.245 \times 10^{-20}\ \text{cm}^3 = 4.816 \times 10^{-19}\ \text{g}$

The total mass of platinum in 100 mL $H_2PtCl_6 \cdot 6H_2O$ solution used for preparing PtNPs is

$m_{\text{total Pt}} = c_{\text{H2PtCl6·6H2O}}\ V_{\text{H2PtCl6·6H2O}}\ M_{\text{Pt}} / M_{\text{H2PtCl6·6H2O}} = 0.0001\ \text{g mL}^{-1} \times 100\ \text{mL} \times 195.05\ \text{g mol}^{-1} / 517.92\ \text{g mol}^{-1} = 3.766 \times 10^{-3}\ \text{g}$

The number of 3.5 nm PtNPs prepared from 100 mL $H_2PtCl_6 \cdot 6H_2O$ solution based on the complete transformation of H_2PtCl_6 to PtNPs is

$N_{\text{PtNPs}} = m_{\text{total Pt}} / m_{\text{an PtNP}} = 3.766 \times 10^{-3}\ \text{g} / 4.816 \times 10^{-19}\ \text{g} = 7.820 \times 10^{15}$

The amount of 3.5 nm PtNPs prepared from 100 mL $H_2PtCl_6 \cdot 6H_2O$ solution is

$n_{\text{PtNPs}} = N_{\text{PtNPs}} / N_A = 7.820 \times 10^{15} / 6.02 \times 10^{23} = 1.30 \times 10^{-8}\ \text{mol}$

The particle concentration of 3.5 nm PtNPs prepared from 100 mL $H_2PtCl_6 \cdot 6H_2O$ solution is

$c_{\text{PtNPs}} = n_{\text{PtNPs}} / V_{\text{H2PtCl6·6H2O}} = 1.30 \times 10^{-8}\ \text{mol} / 100\ \text{mL} = 1.30 \times 10^{-7}\ \text{mol L}^{-1} = 130\ \text{nmol L}^{-1} = 130\ \text{nM}$

C3. Calculation process of the relationship between the H_2S amount and the corresponding decrease of final indicator (TMB_{ox}) amount.

Known conditions:

1) the H_2S concentration: $c_{\text{H2S}} = 100$ nM,

2) the H_2S volume: $V_{\text{H2S}} = 10$ μL,

3) the absorbance (at 650 nm) of the detection solution ($c_{\text{H2S}} = 0$ nM): $A_0 = 1.7092$,

4) the absorbance (at 650 nm) of the detection solution ($c_{\text{H2S}} = 100$ nM): $A_{100} = 0.8810$,

5) the volume of the detection solution: $V_{\text{TMBox}} = 100$ μL

6) the molar absorption coefficient of TMB_{ox}: $\varepsilon_{\text{TMBox}} = 3.9 \times 10^4\ \text{M}^{-1}\text{cm}^{-1}$,

7) the path length of 100 μL detection solution in microplate: $b = 0.3$ cm.

Then, the corresponding concentrations of final indicator (TMB_{ox}) solution toward 0 and 100 nM H_2S based on the Beer-Lambert law ($A = \varepsilon\, b\, c$) are

$c_{\text{TMBox,1}} = A_0 / (\varepsilon_{\text{TMBox}}\ b) = 1.7092 / (3.9 \times 10^4\ \text{M}^{-1}\text{cm}^{-1} \times 0.3\ \text{cm}) = 1.4609 \times 10^{-4}\ \text{M} = 146.09\ \mu\text{M}$,

$c_{\text{TMBox,100}} = A_{100} / (\varepsilon_{\text{TMBox}}\ b) = 0.8810 / (3.9 \times 10^4\ \text{M}^{-1}\text{cm}^{-1} \times 0.3\ \text{cm}) = 0.7530 \times 10^{-4}\ \text{M} = 75.30\ \mu\text{M}$

the corresponding decrease of final indicator (TMB_{ox}) concentration in 100 μL solution toward 100 nM H_2S is

$$\Delta c_{TMBox} = c_{TMBox,1} - c_{TMBox,100} = 146.09\ \mu M - 75.30\ \mu M = 70.79\ \mu M$$

the relationship between the H_2S amount and the corresponding decrease of final indicator (TMB_{ox}) amount is

$$N = (\Delta c_{TMBox}\ V_{TMBox}) / (c_{H2S}\ V_{H2S}) = (70.79\ \mu M \times 100\ \mu L) / (100\ nM \times 10\ \mu L) = 7079$$

D. References

(S1).Li, J.; Yang, Z.; Ren, B.; Liu, G.; Fang, P.; Jiang, Y.; Wu, D.; Tian, Z. *Langmuir* **2006**, *22*, 10372−10379.

(S2).Fang, P.; Duan, S.; Lin, X.; Anema, J. R.; Li, J.; Buriez, O.; Ding, Y.; Fan, F.; Wu, D.; Ren, B.; Wang, Z. L.; Amatore, C.; Tian, Z. *Chem. Sci.* **2011**, *2*, 531−539.

(S3).Bigall, N. C.; Härtling, T.; Klose, M.; Simon, P.; Eng, L. M.; Eychmüller, A. *Nano Lett.* **2008**, *8*, 4588−4592.

(S4).Wu, G.; He, S.; Peng, H.; Deng, H.; Liu, A.; Lin, X.; Xia, X.; Chen, W. *Anal. Chem.* **2014**, *86*, 10955−10960.

(S5).Zhuang, J.; Fu, L.; Lai, W.; Tang, D.; Chen, G. *Chem. Commun.* **2013**, *49*, 11200−11202.

(S6).Clark, S. J.; Segall, M. D.; Pickard, C. J.; Hasnip, P. J.; Probert, M. I. J.; Refson, K.; Payne, M. C. *Z. Kristallogr.* **2005**, *220*, 567−570.

(S7).Perdew, J. P.; Burke, K.; Ernzerhof, M. *Phys. Rev. Lett.* **1996**, *77*, 3865.

(S8).Pfrommer, B. G.; Câté, M.; Louie, S. G.; Cohen, M. L. *J. Comput. Phys.* **1997**, *131*, 233−240.

(S9).Gao, Z.; Xu, M.; Hou, L.; Chen, G.; Tang, D. *Anal. Chim. Acta* **2013**, *776,* 79−86.

(S10). Gao, Z.; Xu, M.; Lu, M.; Chen, G.; Tang, D. *Biosens. Bioelectron.* **2015**, *70*, 194−201.

(S11). Siegel L. M. *Anal. Biochem.* **1965**, *11*, 126−132.

(S12). Jarosz, A. P.; Yep, T.; Mutus, B. *Anal. Chem.* **2013**, *85*, 3638−3643

(S13). Zhang, J.; Xu, X.; Yang, X. *Analyst* **2012**, *137*, 1556−1558.

(S14). Huang, H.; Li, Q.; Wang, J.; Li, Z.; Yu, X.; Chu, P. K. *Plasmonics* **2014**, *9*, 11–16.

(S15). Zhang, J.; Xu, X.; Yuan, Y.; Yang, C.; Yang, X. *ACS Appl. Mater. Interfaces* **2011**, *3*, 2928–2931.

(S16). Montoya, L. A.; Pearce, T. F.; Hansen, R. J.; Zakharov, L. N.; Pluth, M. D. *J. Org. Chem.* **2013**, 78, 6550−6557.

(S17). Deng, H.; Weng, S.; Huang, S.; Zhang, L.; Liu, A.; Lin, X.; Chen, W. *Anal. Chim. Acta* **2014**, *852*,

218−222.

(S18). Hao, J.; Xiong. B.; Cheng, X.; He, Y.; Yeung, E. S. *Anal. Chem*. **2014**, *86*, 4663−4667.

(S19). Yang, S.; Qi, Y.; Liu, C.; Wang, Y.; Zhao, Y.; Wang, L.; Li, J.; Tan, W.; Yang, R. *Anal. Chem*. **2014**, *86*, 7508−7515.

(S20). Liu, B.; Chen, Y. *Anal. Chem*. **2013**, *85*, 11020−11025.

(S21). Lim, C. S.; Das, S. K.; Yang, S. Y.; Kim, E. S.; Chun, H. J.; Cho, B. R. *Anal. Chem*. **2013**, *85*, 9288−9295.

(S22). Cao, X.; Lin, W.; Zheng, K.; He, L. *Chem. Commun*. **2012**, *48*, 10529−10531.

(S23). Huang, Z.; Ding, S.; Yu, D.; Huang, F.; Feng, G. *Chem. Commun*. **2014**, *50*, 9185−9187.

(S24). Mao, G.; Wei, T.; Wang, X.; Huan, S.; Lu, D.; Zhang, J.; Zhang, X.; Tan, W.; Shen, G.; Yu, R. *Anal. Chem*. **2013**, *85*, 7875−7881.

(S25). Wang, X.; Sun, J.; Zhang, W.; Ma, X.; Lv, J.; Tang, B. *Chem. Sci*. **2013**, *4*, 2551–2556

(S26). Chen, W.; Lan, G.; Chang, H. *Anal. Chem*. **2011**, *83*, 9450–9455.

(S27). Yu, Q.; Zhang, K. Y.; Liang, H.; Zhao, Q.; Yang, T.; Liu, S.; Zhang, C.; Shi, Z.; Xu, W.; Huang, W. *ACS Appl. Mater. Interfaces* **2015**, *7*, 5462−5470.

(S28). Liu, S.; Zhang, L.; Yang, T.; Yang, H.; Zhang, K. Y.; Zhao, X.; Lv, W.; Yu, Q.; Zhang, X.; Zhao, Q.; Liu, X.; Huang, W. *ACS Appl. Mater. Interfaces* **2014**, *6*, 11013−11017.

(S29). Tropiano, M.; Faulkner, S. *Chem. Commun*. **2014**, *50*, 4696–4698.

(S30). Ye, Z.; An, X.; Song, B.; Zhang, W.; Dai, Z.; Yuan, J. *Dalton Trans*. **2014**, *43*, 13055–13060.

(S31). Yan, Y.; Yu, H.; Zhang, Y.; Zhang, K.; Zhu, H.; Yu, T.; Jiang, H.; Wang, S. *ACS Appl. Mater. Interfaces* **2015**, *7*, 3547−3553.

(S32). Dai, Z.; Tian, L.; Song, B.; Ye, Z.; Liu, X.; Yuan, J. *Anal. Chem*. **2014**, *86*, 11883−11889.

(S33). Lawrence, N. S.; Jiang, L.; Jones, T. G. J.; Compton, R. G. *Anal. Chem*. **2003**, *75*, 2054−2059.

(S34). Lawrence, N. S.; Jiang, L.; Jones, T. G. J.; Compton, R. G. *Anal. Chem*. **2003**, *75*, 2499−2503.

(S35). Jeroschewski, P. Steuckart, C.; Kuhl, M. *Anal. Chem*. **1996**, *68*, 4351−4357.

(S36). Bitziou, E.; Joseph, M. B.; Read, T. L.; Palmer, N.; Mollart, T.; Newton, M. E.; Macpherson, J. V. *Anal. Chem*. **2014**, *86*, 10834−10840.

(S37). Lawrence, N. S.; Deo, R. P.; Wang, J. *Anal. Chim. Acta* **2004**, *517*, 131−137.

(S38). Doeller, J. E.; Isbell, T. S.; Benavides, G.; Koenitzer, J.; Patel, H.; Patel, R. P.; Lancaster, J. R.; Darley-Usmar, V. M.; Kraus, D. W. *Anal. Biochem*. **2005**, *341*, 40−51.